https://rbgeomorfologia.org.br/
*ISSN 2236-5664*

**Revista Brasileira de Geomorfologia**

v. 26, nº 4 (2025)

http://dx.doi.org/10.20502/rbg.v26i4.2680

*Research Article*

# Impact of the input of mining tailings on the mobility of the coastline at the mouth of the Doce River-ES

## *Impacto do aporte do rejeito de mineração sobre a mobilidade da linha de costa na desembocadura do rio Doce-ES*

**Branco Eguchi [1], Maite Noda Zanotti [2], Jacqueline Albino [3], Pablo Medeiros Jabor [4], Giseli Modolo Vieira Machado [5], Luiz Henrique Sielski de Oliveira [6], Lucas Bermudes de Castro [7], Alexandre Burini [8]**

[1] Universidade Federal do Espírito Santo, Departamento de Oceanografia, Vitória, Brasil. bmeguchi@hotmail.com
ORCID: https://orcid.org/0000-0001-9795-780X
[2] Universidade Federal do Espírito Santo, Departamento de Oceanografia, Vitória, Brasil. maitenoda@gmail.com
ORCID: https://orcid.org/0009-0009-4112-3940
[3] Universidade Federal do Espírito Santo, Departamento de Oceanografia, Vitória, Brasil. albino.jacqueline@gmail.com
ORCID: https://orcid.org/0000-0003-2890-9227
[4] Instituto Jones do Santos Neves, Vitória, Brasil. pmjabor@gmail.com
ORCID: https://orcid.org/0000-0002-3580-8937
[5] Universidade Federal do Espírito Santo, Departamento de Oceanografia, Vitória, Brasil. giselimodolo@gmail.com
ORCID: http://orcid.org/0000-0002-2169-4123
[6] Universidade Federal do Espírito Santo, Departamento de Oceanografia, Vitória, Brasil. luizion@gmail.com
ORCID: https://orcid.org/0000-0002-5069-5619
[7] Universidade Federal do Espírito Santo, Departamento de Oceanografia, Vitória, Brasil. lucasbdec@gmail.com
ORCID: https://orcid.org/0000-0002-1992-7813
[8] Universidade Federal do Espírito Santo, Departamento de Oceanografia, Vitória, Brasil. alexandreburini@hotmail.com
ORCID: https://orcid.org/0009-0006-6904-6041

Received: 03/04/2025; Accepted: 28/07/2025; Published: 24/09/2025

**Abstract:** The collapse of Mariana dam in Minas Gerais, Brazil is regarded as the largest disaster of its kind in history. The material, composed of an extremely fine fraction of sediments, traveled more than 660 km until reaching the river mouth, near the village of Regência, ES. This study aims to quantify shoreline changes in response to tailings input, using satellite imagery. Additionally, it investigates triggers responsible for these changes, such as river discharge, precipitation and littoral drift. The study also evaluates, through topographic and granulometric monitoring, the current morphodynamic equilibrium of the beaches affected by tailing deposition. The results indicate shoreline erosion in the period following the tailing arrival. That period was characterized by normal precipitation and littoral drift, but with significantly low river discharge. Erosion persisted during the current period, even with an increase in river discharge. Moreover, beach monitoring revealed trends of granulometric reduction and increase in mud content. In conclusion, acute impacts were detected as an immediate response to tailing arrival. Along with chronic impacts, recent inputs of tailing mud were observed, deposited along the river.

**Keywords:** River discharge; Precipitation; Coastal drift; Equilibrium profile; Mud on the shore.

**Resumo:** O rompimento da barragem de mineração em Mariana-MG ficou marcado como o maior da história. O material composto por uma fração extremamente fina de sedimentos, percorreu mais de 660 km até atingir a desembocadura do rio, na vila de Regência-ES. O presente artigo visa determinar variações na linha de costa em resposta à chegada do rejeito, por meio de imagens de satélite. Além de investigar gatilhos de tais alterações, como descarga fluvial, precipitação e deriva litorânea. Por fim, avalia o equilíbrio morfodinâmico atual das praias afetadas pelo aporte do rejeito, por meio de monitoramento topográfico e granulométrico. Os resultados apontam erosão da linha de costa no intervalo subsequente à

chegada do rejeito ao litoral. Este período é marcado por padrões normais de precipitação e deriva litorânea, porém, com redução significativa da descarga fluvial. Para o período atual, a erosão da linha de costa persiste, mesmo com aumento da descarga fluvial. Além disso, o monitoramento mostra tendências de redução granulométrica e aumento no teor de lama. Em conclusão, ficam evidenciados impactos agudos, como resposta imediata à chegada do rejeito. Além de impactos crônicos, relacionados ao aporte recente do rejeito depositado ao longo do rio.

**Palavras-chave:** Descarga fluvial; Precipitação; Deriva litorânea; Perfil de equilíbrio; Lama na antepraia.

## 1. Introduction

Temporal variations in the morphology of sandy ocean beaches are controlled by longitudinal and transverse sediment transport. Longitudinal changes are characterized by the mobility of the coastline and represent longer time scales (months, years, or decades). In contrast, transverse modifications represent the dynamics of the beach transverse profile, representing short-time-scale processes (hours, days, or weeks) (Karunarathna *et al*., 2016). Morphological balance on sandy ocean beaches is defined by the balance between sediment and wave energy. In this sense, beaches with coarse sediments are associated with high slope and low wave energy. As beaches with fine sediments, they have low slope and high wave energy (Bascom, 1951; Silvester and Hsu, 1997; Wright and Short, 1984). Changes in the wave energy pattern or sediment granulometry tend to trigger disturbances in the shape of the beach, altering the morphodynamic balance (Bird, 2008; Short and Jackson, 2013; Davidson-Arnott, Bauer and Houser, 2019).

According to the Public Prosecutor's Office of the state of Minas Gerais (MPMG), on November 5, 2015, about 60,000,000 m³ of iron ore tailings were dumped in the Doce River basin as a result of the collapse of the Fundão dam, controlled by the mining company Samarco, in Mariana, MG. According to the State Institute of Environment and Water Resources of Espírito Santo (IEMA-ES), after 17 days, the final destination of this material was the mouth of the Doce River, located in the village of Regência, part of the municipality of Linhares, ES. Albino, Contti Neto and Oliveira (2016) describe the beaches on the Doce River plain as exposed to waves and composed of medium to coarse siliciclastic sands. Therefore, the iron ore tailings that reached the coastal region represented the contribution of muddy sediment, extremely fine when compared to the sediment previously present in this region (Do Carmo em Mariana-MG. De*et al*., 2017; Quaresma *et al*., 2020). In addition, in the early stages of the arrival of this material, there was a reduction in the density of the surface layer of the bottom deposits near the river mouth, facilitating its remobilization by wave action directed towards the coastal zone (Quaresma *et al*., 2020; Vinzon *et al*., 2024). Estimates indicate that approximately half of the mining tailings are trapped in reservoirs and along the Doce River channel, so new mud pulses are expected in the coastal zone during periods of high river discharge (Vinzon *et al*., 2024).

Although the physical impacts generated by the change in sediment composition in the coastal region are recognized, due to the arrival of mining tailings (Sanchez *et al*., 2018; Franco *et al*., 2024), most coastal impact studies address changes in the concentration of chemical elements and their consequences for the biotic and abiotic environment (Richard *et al*., 2020; Schettini and Hatje, 2020; Costa *et al*., 2021; Costa *et al*., 2022; Marques *et al*., 2022; Silva *et al*., 2022). However, Souza *et al*. (2022) and Brahim *et al*. (2024) highlight the importance of the control exerted by the morphodynamics of the beaches adjacent to the Doce River in the accumulation of chemical elements and biological diversity. Thus, they emphasize the importance of evaluating morphodynamic changes on the beaches generated by the contribution of muddy material from mining tailings.

The impact of mud input on sandy beaches is commonly discussed in terms of wave energy attenuation and shoreline progradation (Wells and Roberts 1980; Roberts *et al* 1989; Huh *et al*., 1991; Calliari *et al*., 2007). However, near the mouth of the Doce River, the progradation pattern of the coastline results from sedimentary transport generated by wave action (Dominguez, Bittencourt and Martin, 1983; Albino, Girardi and Do Nascimento, 2006; Oliveira, Albino and Venâncio, 2015; Albino, Contti Neto and Oliveira, 2016). Thus, the presence of mud can have the opposite effect to that expected and trigger erosive processes along the coastline adjacent to the river mouth. In addition to reducing wave action, the presence of mud can also trap sandy sediments in the foreshore region, limiting its transport and triggering erosive processes on the shoreline (Muehe et al., 2010).

In view of this particular contrast, the objective of the present study is to elucidate the impacts generated by the mud input in the coastal zone adjacent to the mouth of the Doce River through the investigation of the fluvial discharge of the Doce River in response to precipitation in its watershed and the sediment transport generated by

littoral drift. This will permit identifying patterns responsible for altering the mobility of the coastline before and after the arrival of the mining tailings on the coast. In addition, it addresses the current morphodynamic balance of the beaches as a way to assess the impacts of the recent input of mining tailings. The analyses presented allow a multi-scale evaluation of coastal processes (Karunarathna *et al*., 2016).

## 2. Area of Study

According to Cupolillo, De Abreu and Vianello (2008), rainfall in the Doce River basin is mainly controlled by frontal systems and tropical convection, characterized by a rainy season between October and March and a dry period from April to September.

The most representative waves in this region occur from the E/NE and S/SE quadrants, generated, respectively, by the South Atlantic High (South Atlantic Subtropical Anticyclone) and frontal systems originating at higher latitudes (Pianca; Mazzini and Siegle, 2010). Storm waves have heights between 2.5 and 3.0 m periods between 13 and 15 s (Eguchi and Klumb-Oliveira, 2023). The tidal regime is characterized by a micro-tide with an average height of 0.78 m, ranging from 0.1 to 1.5 m (DHN, 2025).

Oliveira and Quaresma (2017) state that the contribution of the Doce River is responsible for more than 70% of the terrigenous sediment on the continental shelf, reaching 10,000,000 t of sediment during the summer. According to Vieira *et al.* (2019), due to the terrigenous input, the concentration of carbonate sediments on the continental shelf adjacent to the mouth of the Doce River is lower than the entire shelf, predominantly carbonate, of the state of Espírito Santo, with values below 30%. The authors noted the presence of this terrigenous mud from the contribution of the Doce River up to the 20m isobath (Figure 1).

According to Albino and Suguio (2010), beaches near and north of the mouth of the Doce River have fine to coarse sand. In contrast, beaches south of the mouth receive coarse-grained siliciclastic sediments (Albino *et al*., 2016). This composition is a reflection of the redistribution of the fluvial input along the foreshore, which in turn is strongly influenced by the littoral drift generated by the angle of incidence of the waves in the swash zone (Vinzon et al., 2024). The net transport of the sedimentary load of the river is towards the northern flank of the deltaic plain, by means of currents resulting from interactions of the incident waves with the bathymetry and local coastline (Bittencourt *et al*., 2007; Oliveira, Albino and Venâncio, 2015). The transport varies in magnitude between 80,000 and 120,000 $m^3$/year and has an increase in its potential north of the mouth (Oliveira, Albino and Venancio, 2015). According to the authors, although waves from the N, NE and E are more frequent, the littoral drift has net northward transport due to the high energy of the waves from the S and SE.

Albino, Girardi and Do Nascimento (2016) indicate that the coastline adjacent to the mouth of the Doce River is characterized by progradation of the coastline due to the intense sedimentary input and the effect of a hydraulic jetty generated by river discharge, favoring the accumulation of sediments brought by littoral drift in the region (Dominguez, Bittencourt and Martin, 1983; Oliveira, Albino and Venancio, 2015; Albino, Contti Neto and Oliveira, 2016).

The stretch of coastline studied is about 16 km long, covering the north and south flanks of the Doce River plain, in addition to 3 fixed monitoring stations located in Povoação (North), Regência (Mouth) and in the Biological Reserve of Comboios (South). (Figure 1; Table 1).

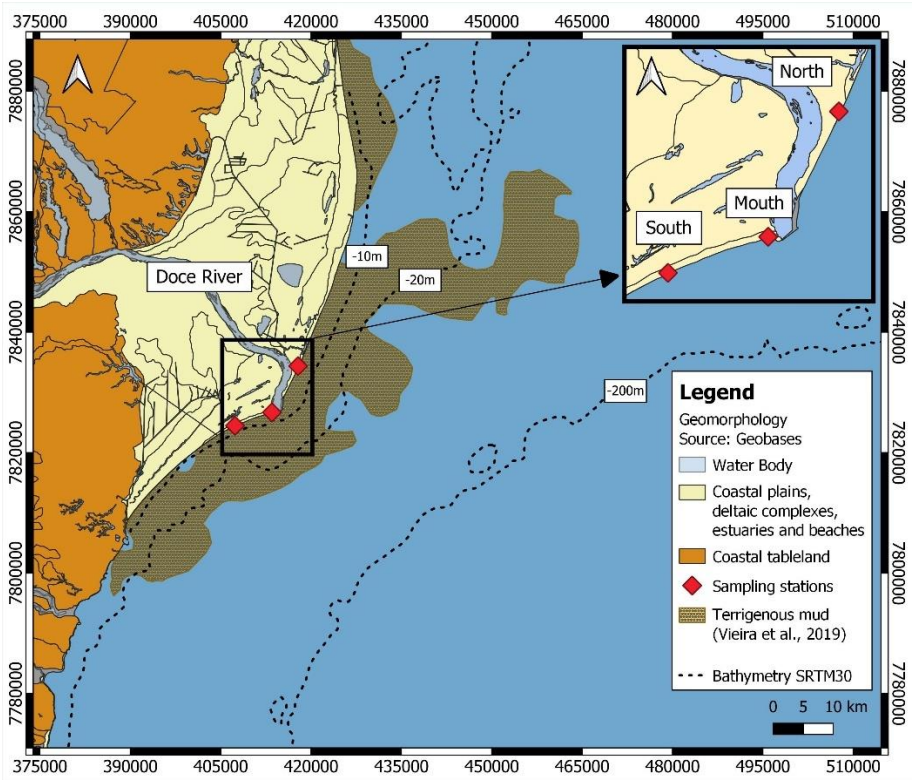


**Figure 1.** Geomorphology and location of the study area and sampling stations.

**Table 1.** UTM position of the sedimentary and bathymetric sampling stations.

| Station | Location | X | Y | Distance from mouth |
|---|---|---|---|---|
| North | Povoação | 417840.0 | 7834371.4 | 7.5 km |
| Mouth | Regência | 413504.3 | 7826697.9 | < 1 km |
| South | REBio Comboios | 407367.1 | 7824486.8 | 8 km |

## 3. Materials and Methods

### *3.1 Precipitation and river discharge*

Precipitation data in the Rio Doce basin were obtained through the Hidroweb platform, part of the National Water Resources Information System (SNIRH) and coordinated by the National Water Agency (ANA). The information consists of measurements of the monthly averages carried out at 80 stations within the drainage area of the basin in the intervals 2008-2014 (6 years), 2014-2020 (6 years) and 2020-2023 (3 years) (Figure 2). The average fluvial discharge of the Doce River was evaluated by means of time series between the same intervals, based on the compilation of monthly averages of the Colatina river gauging station (code 56994500), managed by ANA in partnership with the Geological Service of Brazil (CPRM). The drainage area of the Doce River in this region is 76,400 km²; the main tributaries with mouths located in the city add up to an additional drainage area of 3,006 km².

To enable the comparison between the different time intervals, accumulated average values of precipitation and annual discharge were calculated (Eq. 1).

$$V_{aa} = \frac{1}{n}\sum_{1}^{n}\sum V_{a_n} \quad (1)$$

where $V_{aa}$ represents the accumulated annual discharge or precipitation, n is the number of years of each interval and $V_{a_n}$ the monthly discharge or precipitation measured in each year.

*3.2 Wave-generated littoral drift*

The wave data is part of the ERA5 global reanalysis, made available by the European Centre for Medium-Range Weather Forecasts (ECMWF) (Hersbach *et al*., 2020) and provides significant heights, peak periods and average wave directions, assessed on the continental shelf near the 1300 m isobath.

The present study evaluated the wave conditions for the 2008-2014, 2014-2020 and 2020-2023 intervals with a spatial resolution of 0.25° x 0.25° and a temporal resolution of 1 hour (Figure 2).

To validate the data from the ERA5 model, the modeled wave information was compared to information measured *in situ*, obtained from the Vitória buoy, part of the National Buoy Program (PNBOIA). The buoy is anchored at a depth of 200 m, approximately 21 km from point ERA5, and provides information on significant wave height, peak period and average direction between 2015 and 2017 (Figure 2). Table 2 presents the bias and the Root Mean Squared Errors (RMSE) between the measured and modeled wave data. The comparison indicates that the ERA5 wave data satisfactorily represent the pattern of significant height (Hs) and peak period (Tp) measured *in situ*. The average direction discrepancy (Dm) may be linked to the difference in depth between the points, as a consequence of refraction and diffraction processes on the continental shelf.

**Table 2.** Statistical parameters of Root mean squared Error (RSME) and bias between measured (PNBOIA) and modeled (ERA5) wave data.

| | **HS(m)** | **Tp(s)** | **Dm(°)** |
|---|---|---|---|
| RSME (m) | 0.2 | 1.4 | 20.3 |
| Bias (m) | 0.1 | 0.5 | 9.8 |

The calculation of the transport generated by the coastal drift for the intervals 2008-2014, 2014-2020 and 2020-2023 was carried out using Eq. 2 (Kamphuis, 2002), taking into account the peak period (Tp), granulometric median (D50), slope of the beach face (mb), angle of incidence of the waves on the coastline ($\theta_b$) and height of wave break (Hb). The wave break height was estimated from Eq. 3 (Le Mehaute and Koh, 1967), based on the height and length of waves *offshore* (Ho and Lo, respectively) and the slope of the seabed (S). To solve the difficulty in determining the orientation of the coastline, especially in the region of the mouth of the Doce River, the orientation of the 10 m isobath was used as a reference. This boundary represents a region more stable than the coastline itself and close to the depth of closure ($H_f$ ~ 9m), determined based on ERA5 wave data through Eq. 4 (Hallermier, 1981). Therefore, it can be considered a zone of strong wave influence on the seabed in terms of remobilization of the bottom and generation of currents.

$$Q = 2.22{H_b}^2 * {T_p}^{1.5} * {m_b}^{0.75} * {D_{50}}^{-0.25} * sen^{0.6}(2\theta_b) \quad (2)$$

$$H_b = H_o * 0.76 * S^{0.14} * \left(\frac{H_o}{L_o}\right)^{-0,25} \quad (3)$$

$$H_f = 2 * Hs + 11\sigma \quad (4)$$

where Hs represents the significant wave height and $\sigma$ the standard deviation of the database.

Similar to the river discharge data, accumulated annual transport was calculated (Eq. 5), in order to overcome the difference in time intervals between the periods analyzed.

$$Q_{aa} = \frac{1}{n}\sum_{1}^{n}\sum Q_{a_n} \quad (5)$$

where $Q_{aa}$ represents the accumulated annual transport, n is the number of years of each interval and $Q_{a_n}$ the hourly transport in each year.

In order to determine changes in hydrological and oceanographic parameters between the 2008-2014, 2014-2020 and 2020-2023 intervals, the non-parametric Kruskal-Wallis test was performed, indicated for comparison of two or more populations (Gilbert, 1987).

### *3.3 Mesoscale shoreline mobility*

The position of the coastline was defined using the line of vegetation in contact with the beach as an indicator, which is an easily detectable indicator present throughout the coastline (Boak and Turner, 2005). The images used were produced by the Landsat 8 satellite, operated by the United States Geological Survey (USGS) in conjunction with the National Aeronautics and Space Administration (NASA) and obtained through *Google Earth* software. Images from the years 2008, 2014, 2020 and 2023 with a resolution of 30 m/pixel were chosen, covering the region between the North and South monitoring stations (Figure 2). Rates of change were calculated using the *Digital Shoreline Analysis System* (DSAS), widely applied for this purpose (Thieler and Danforth, 1994; Baig *et al*., 2020; Gharnate, Taouali and Mhammdi, 2024). Within DSAS, the analysis of the variation of the coastline was conducted based on transects perpendicular to the coastline, spaced 100 meters apart along the analyzed coastline. The rate of change of the coastline in the 2008-2014 interval represents the mobility before the arrival of the mining tailings to the coastal zone. Between 2014 -2020, the rate of variation refers to mobility after the entry of muddy material from the tailings into the coastal system. Between 2020 – 2023, variation of the coastline represents the current scenario.

### *3.4 Morphodynamic monitoring*

Fieldwork was carried out every six months between 2018 and 2023, totaling 15 campaigns (Table 3). Sandy sediments collected in the swash and surf zones and 5 and 10 m isobaths and were analyzed for granulometry by dry sieving the -2 and 4 φ fractions (4 and 0.063 mm). To determine the grain size distribution and granulometric composition of the muddy sediments, the wet sieving of the entire sample was carried out using the 4 φ mesh (0.063 mm). Organic matter was removed using hydrogen peroxide on a heating plate in the fume hood. The determination of the granulometry was performed by Malvern laser granulometer. Finally, the mean diameter (MD) was calculated for each sampled region based on Wentworth's (1922) particle size classification. The trend of increase or decrease in the average diameter and mud content was calculated using the Mann-Kendall non-parametric statistical test, widely used in the analysis of time series trends (Gilbert, 1987; Silva *et al*., 2010; Lopes and Silva, 2013).

The bathymetry was surveyed simultaneously with the sediment collection along profiles aligned with the collection points by means of single beam echobathymetry with operating frequencies of 210/33Khz, installed in a vessel equipped with GNSS/GPS positioning. In addition, bathymetric mapping was carried out in the foreshore region adjacent to the mouth of the Doce River in two campaigns in 2023. The surveyed area comprised the beginning of the surf zone to 10 m depth, following lines parallel to the coast that extend about 8 km to the south and north of the mouth of the river, with about 80 m spacing between them (Figure 2).

**Table 3.** Dates of sediment and bathymetry collections carried out between 2018 and 2023, marked with 'x'.

| Dates | Grain size | | | Bathymetry | | |
|---|---|---|---|---|---|---|
| | South | Mouth | North | South | Mouth | North |
| Sep/18 | x | | x | x | | x |
| Dec/18 | x | | x | x | | x |
| Apr/19 | x | | x | x | | x |
| Jul/19 | x | | x | x | | x |
| Nov/19 | x | x | x | | | |
| Dec/19 | | | | x | x | x |
| Jan/20 | x | x | | x | x | x |
| Feb/20 | x | x | x | x | x | x |
| Jan/21 | x | x | x | x | x | x |
| Jul/21 | x | x | x | x | x | x |

| | | | | | | |
|---|---|---|---|---|---|---|
| Jan/22 | | | x | | | |
| Feb/22 | x | x | | x | x | x |
| Aug/22 | x | x | x | | | |
| Sep/22 | | | | x | x | x |
| Jan/23 | | | | x | x | x |

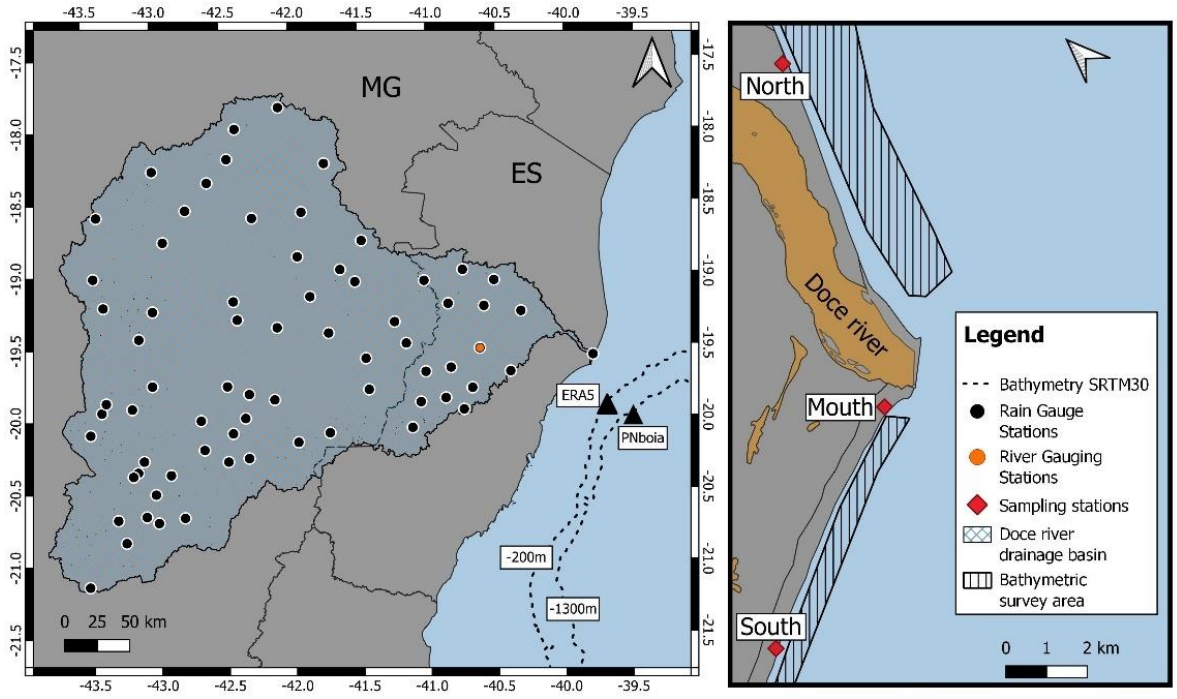


**Figure 2.** Area of the Doce River drainage basin and location of the ANA rain gauge and river gauging stations (left). Location of the bathymetric/sedimentary monitoring stations and bathymetric survey area (right).

To determine the ideal shape of a beach transverse profile in equilibrium, Dean (1991) proposes Eq. 6, which takes into account the average granulometry of the beach face by means of scale parameter A (Figure 3). The comparison of the measured profile with the calculated equilibrium profile (PPE) was performed from a mean profile, determined by polynomial regression of all bathymetric data collected between 2018-2023.

$$h = A * y^{2/3} \tag{6}$$

where h is the depth of the submerged profile, A is a scale parameter based on particle size and y is the horizontal distance of the submerged profile.

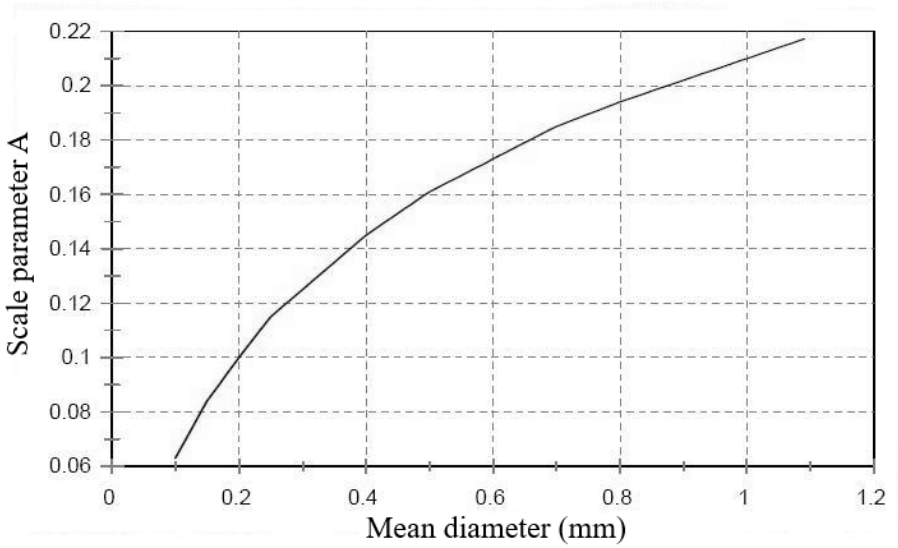


**Figure 3.** Variation of the scale parameter A in relation to the average diameter of sediment collected on the beach face (adapted from Dean, 1991).

## 4. Results

### *4.1 Precipitation and River Discharge*

During the period before the collapse (2008-2014), precipitation and discharge had accumulated annual averages of 5,500 mm and 96,000 m³/s, respectively. In the period after the collapse (2014-2020), there is a reduction of approximately 16% in the average annual accumulated precipitation, falling to 4.600 mm. Discharge, in contrast, shows a drop of almost 47%, reaching the average annual accumulation of 51,000 m³/s. During the years 2020 and 2023, the average annual accumulation of precipitation and discharge return to the levels before the collapse, with values of 5.600 mm and 87,000 m³/s, respectively (Figure 4).

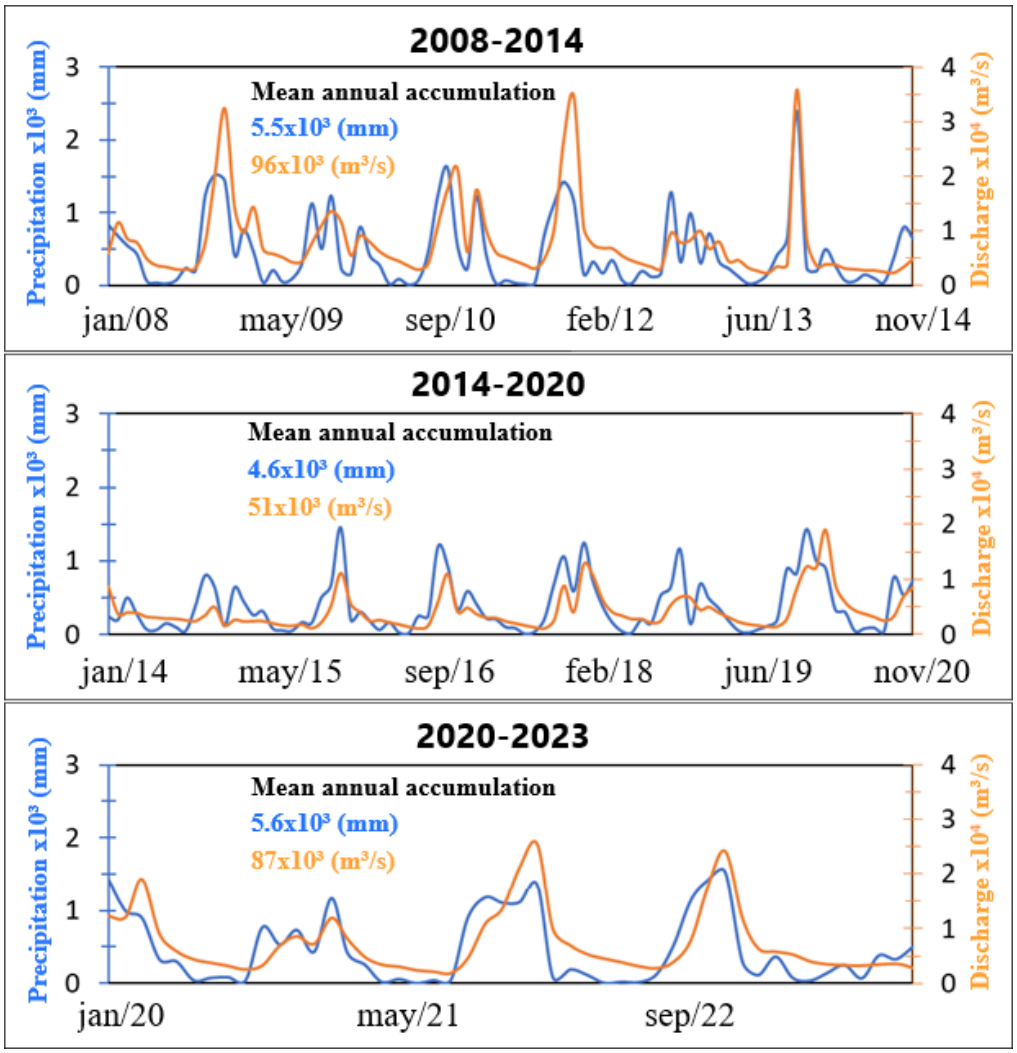


**Figure 4.** Monthly time series of rainfall (precipitation) in the drainage area of the Doce River basin (blue) and river discharge measured by the Colatina-56994500 river gauging station (orange) for the intervals 2008-2014 (top), 2014-2020 (middle) and 2020-2023 (bottom). Values of the accumulated annual rainfall and discharge averages in blue and orange, respectively.

*4.2 Wave-generated littoral drift*

At the North monitoring station, the net transport is to the north, showing the highest values and smallest variations compared to the other regions. Between the 2008-2014 and 2014-2020 intervals, there is a reduction of 1%, while transport reduces 2% between the 2014-2020 and 2020-2023 intervals. In this region, there is a strong predominance of northward transport and insignificant inversions to the south (Figure 5A). At the Mouth station, transport is preferentially to the north, with a 21% decrease between the 2008-2014 and 2014-2020 intervals, and a 24% increase during the 2020-2023 period. In this sector, the balance of the residual transport to the south and north was observed, but those to the north had higher intensities (Figure 5B). The sedimentary transport generated by wave action at the South station was southward with the lowest intensities among all the stations analyzed and brief but intense reversals of direction to the north. Net transport increased by 52% from 2008-2014 to 2014-2020 and decreased by 40% between 2014-2020 and 2020-2023 (Figure 5C).

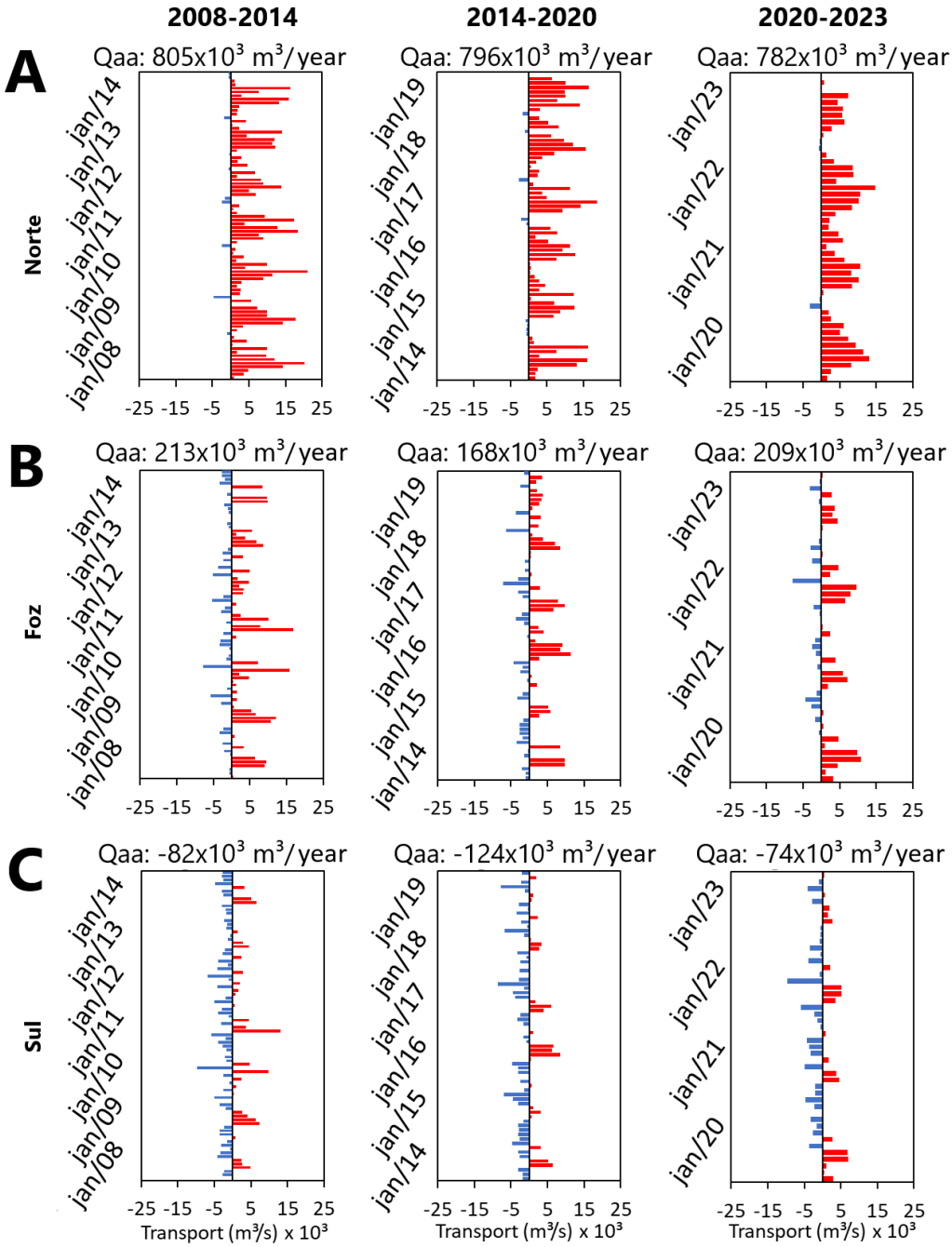


**Figure 5.** Monthly time series and cumulative annual longitudinal transport values calculated for the North (A), Mouth (B) and South (C) stations during the periods 2008-2014 (left), 2014-2020 (middle) and 2020-2023 (right). Negative (positive) values in blue (red) indicate transportation to the south (north).

According to Table 4, the results of the *Kruskall-Wallis* statistical test indicate that only the river discharge presents significant differences between the analyzed intervals. Figure 6 shows accumulated discharge curves over each interval, showing the differences between them. Although the current interval (2020-2023) is smaller than the others, the slope of the curve shows that the behavior of the discharge is similar to the period before the dam collapse (2008-2014). In the period after the dam collapse (2014-2020), it presents a less steep curve, translating into lower river discharges occurring in this interval.

**Table 4.** Results of the Kruskall-Wallis statistical test of similarity for discharge, precipitation and coastal drift variables between the intervals 2008-2014, 2014-2020 and 2020-2023.

| Kruskall-Wallis Test | H | Hc | p |
|---|---|---|---|
| North bank drift | 0 | 0 | 1 |
| Mouth Drift | 0 | 0 | 1 |
| South bank drift | 0 | 0 | 1 |
| Precipitation | 0.2 | 0.2 | 0.9 |
| Discharge | 34.9 | 34.9 | 0 |

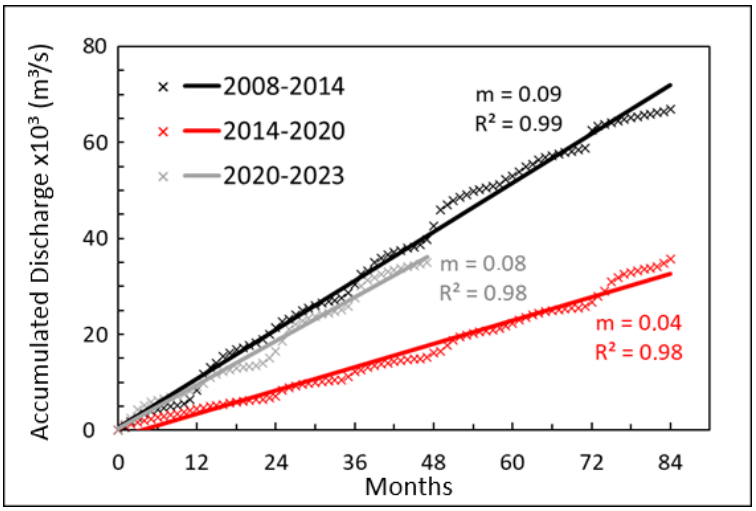


**Figure 6.** Accumulated river discharge curves for the 2008-2014 (Black), 2014-2020 (Gray) and 2020-2023 (Red) intervals. The curves were obtained through linear regression (Lines) of the monthly average discharge data measured by the Colatina-56994500 river gauging station ("x" markers). The parameters m and $R^2$ represent the slope and the regression coefficient for each line.

### *4.3 Modification of the coastline*

In the interval prior to the dam collapse (2008-2014), there was general stability of the coastline on the north and south banks of the river mouth. However, low and medium progradation, between 6 and 18 m, is observed in the vicinity of the mouth and in the portion between the Mouth and South stations, where the 10 m isobath approaches the coastline (Figure 7).

In the interval after the rupture (2014-2020), the coastline at the northern end of the study area remains stable, while the southern end starts to show low and moderate progradation, between 6 and 18 m. In the south and north region of the mouth, erosive processes are medium (12 to 18 m) to high (>18 m). The portion between the South and Mouth stations, previously prograding, now shows stability and low erosion between 6 and 12 m (Figure 7).

The current period (2020-2023) shows a pattern of shoreline mobility similar to the interval after the breach (2014-2020). The coastline in the extreme north of the study area continues to show stability. The progradation at the extreme southern end of the study area intensified and expanded along the coastline towards the mouth. Near the mouth, the behavior continues as an average erosion between 12 and 18 m, with an intensification on the south bank of the river (Figure 7).

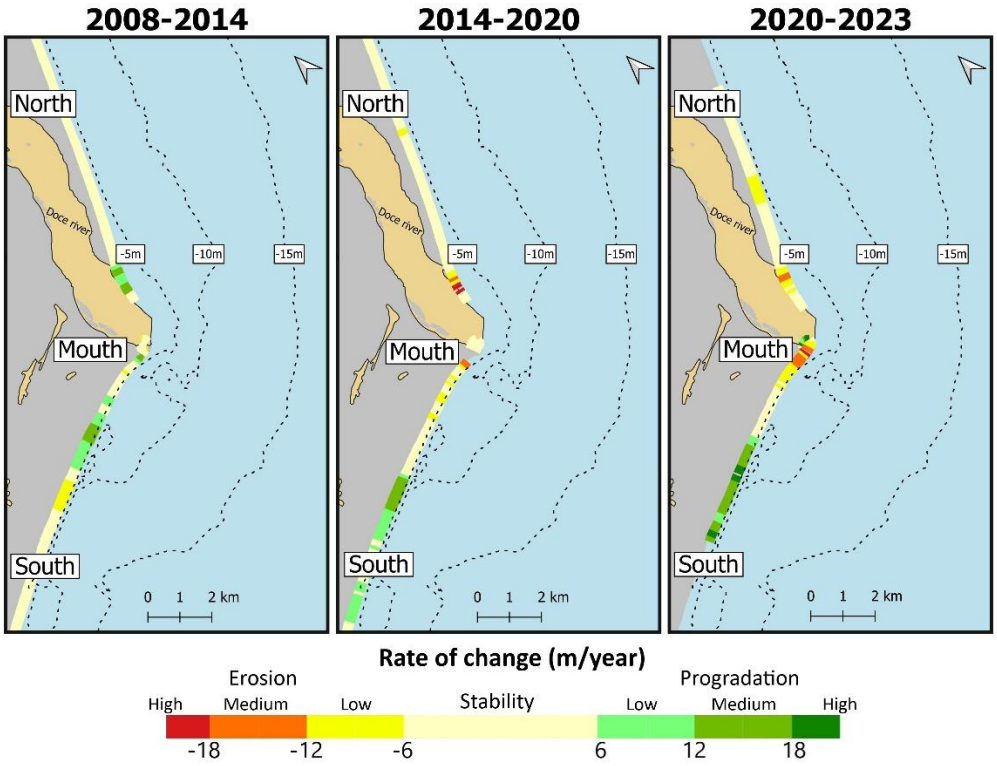


**Figure 7.** Rates of change of the coastline calculated from satellite imagery for the intervals 2008-2014 (Left), 2014-2020 (Center) and 2020-2023 (Right). The dashed lines represent the 5 m, 10 m and 15 m isobaths measured from the detailed survey carried out by means of a dual-frequency single-beam echosounder**.**

*4.4 Morphodynamic equilibrium*

Granulometry indicates the presence of coarse sands at the shoreward-most sampling site (Swash Zone) at each of the three stations, although the North had slightly coarser grains, tending toward very coarse sand. On the shallow foreshore (surf zone), the North and Mouth profiles have sands ranging from very coarse to medium, while at the South station, coarse to medium sands predominate. At the 5 m isobath, very fine sand predominated at the North station and fine to medium sand at the Mouth and South stations. At this isobath, the South station presents greater variability and coarser grains when compared to the others. The samples from the 10 m isobath show the greatest variability compared to the other depths for all seasons. The North station has the finest grain sizes among the stations, ranging from very fine sand to medium silt. At the Mouth station, the granulometry varies from fine sand to medium silt. At the South station, it comprises from fine sand to fine silt. In general, the 10 m isobath showed a tendency toward finer grain sizes along the gradient from south to north (Figure 8A).

The mud content in the samples collected in the swash and surf zones showed values very close to zero. Samples collected at 5 m depth show a spatial gradient with an increase in the percentage of mud from south to north. The North profile has an average content of 61% and a maximum of 98%. In the Mouth profile, the mud content was close to 4%. Despite a single high measurement (~55%), the mud content at the South station is practically nil in the other samples. The spatial gradient of mud content is similar to the particle size, with values increasing from the South to the North station (Figure 8B).

According to the normalized Mann-Kendall statistical test (Table 5), the North profile shows strong tendency of an increase in the mud content and reduction in the average diameter of the sediments at the 5 m isobath. The South profile shows a moderate trend towards a reduction in the mean diameter of the sediments of the surf zone and a strong reduction in the mud content at the 10 m isobath.

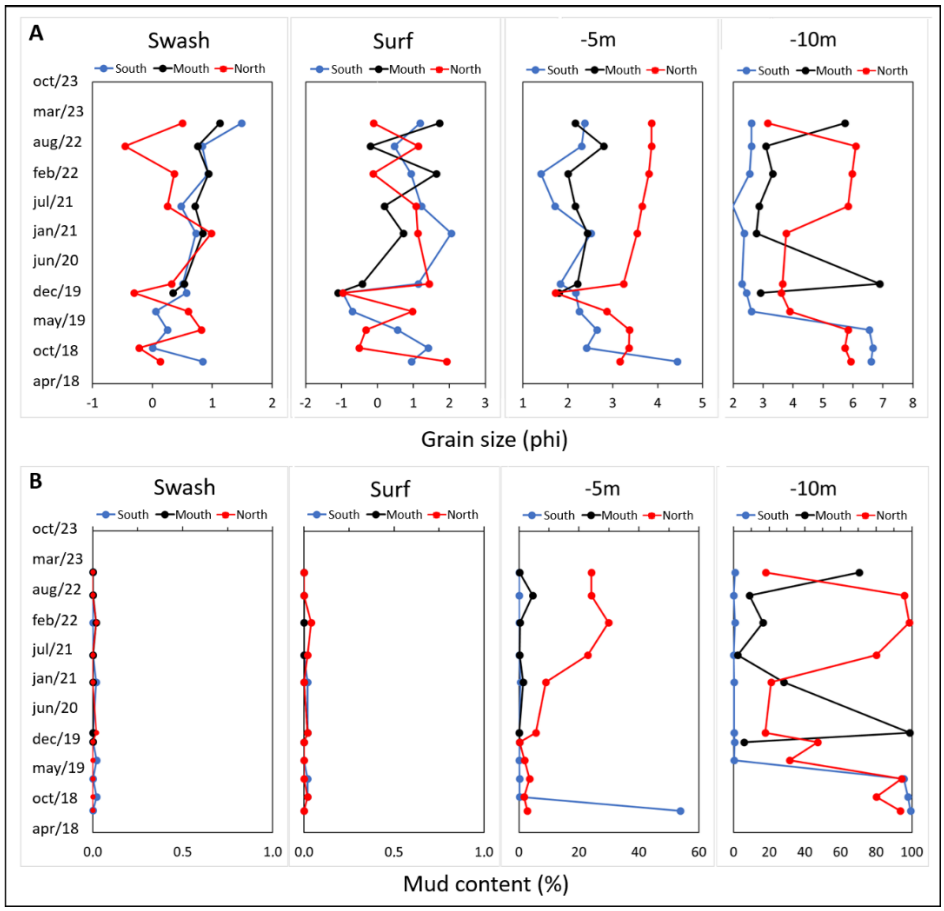


**Figure 8.** Time series of the mean diameter (A) and mud content (B) of sediment samples collected between 2018 and 2023 in the regions of the lower face (Swash zone), shallow foreshore (Surf zone) and 5 and 10 m isobaths.

**Table 5.** Results of the Mann-Kendall statistical test to determine trending increases (red) or decreases (blue) of the mean diameter of the grains in phi (DM) and mud content (%) between the years 2020 and 2023 along the swash and surf zones, and the 5 and 10 m isobaths.

| | **p Mann-Kendall** | | | **S Mann-Kendall Normalized** | | |
|---|---|---|---|---|---|---|
| Parameters | South | Mouth | North | South | Mouth | North |
| DM Swash | 0.04 | 0.02 | . | 0.8 | 0.4 | . |
| DM Surf | . | 0.04 | . | . | 0.4 | . |
| DM 5 m | . | . | 0.01 | . | . | 0.9 |
| DM 10 m | . | . | . | . | . | . |
| %Mud Surf | . | . | . | . | . | . |
| %Mud 5 m | . | . | 0.01 | . | . | 1.0 |
| %Mud 10 m | -0.002 | . | . | -0.8 | . | . |

| **Standardized Mann Kendall S scale** | | | | | | |
|---|---|---|---|---|---|---|
| Tendency | Reduction | | | Increase | | |
| | Low | Average | High | Low | Average | High |
| Intervals | S ≥- 0.4 | -0.4 > S ≥- -0.8 | S < -0.8 | S ≤ 0.4 | 0.4 < S ≤ 0.8 | S > 0.8 |

The average profile at North station profile shows erosion in relation to the equilibrium profile (PPE) up to approximately the depth of 9 m, although the slope of both is similar. Beginning at 9 m depth, there is a strong inflection of the average profile and it begins to show accretion in relation to the PPE, with depths up to 6 m shallower than the calculated PPE (Figure 9A). The average profile at the Mouth station showed accretion compared to the PPE in the first meters of depth, increasing until a depth of approximately 9 m. Although there is a difference in depths, both profiles have a similar slope up to approximately 12 m depth (Figure 9B). In Figure 9C,

the average profile shows erosion in relation to the PPE starting at 2 m depth at the South station. This pattern intensifies at depths greater than 5 m, where the similarity in the slope of the profile ceases, with the average profile becoming steeper.

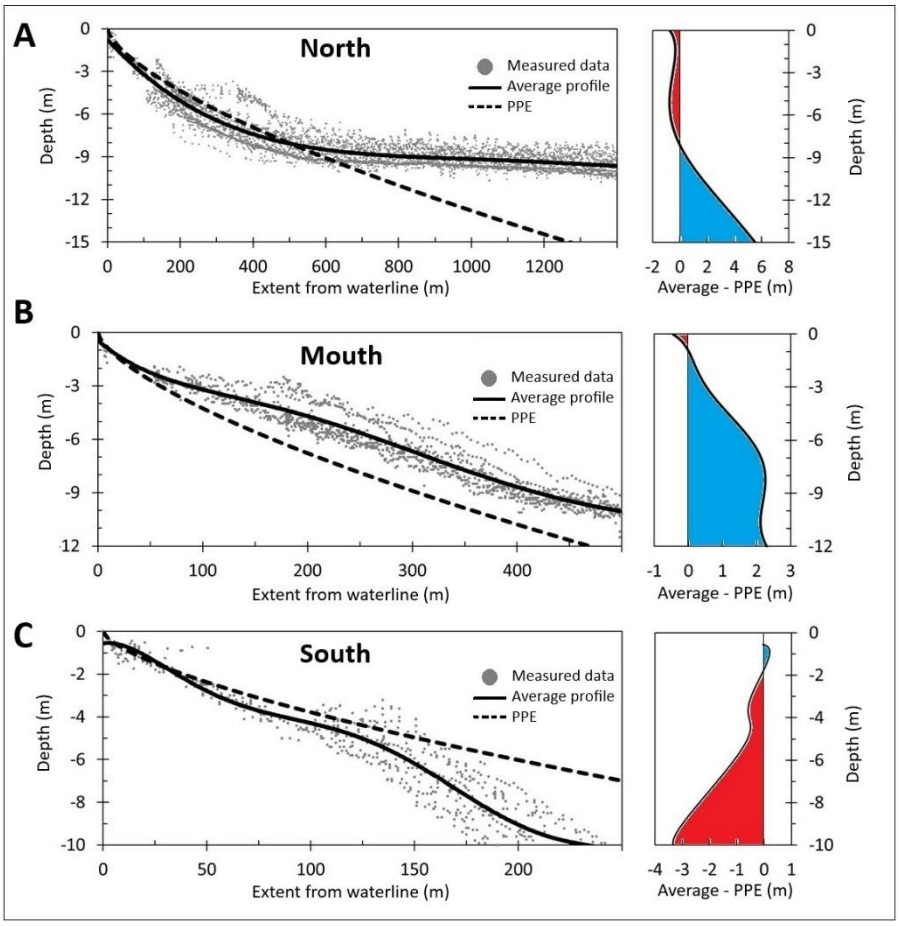


**Figure 9.** Left: Average profiles (Solid line) calculated based on polynomial approximation of bathymetric points surveyed between 2018 and 2023 (Gray dots). Equilibrium beach profiles (PPE) calculated based on the particle size of the beach face collected during the 2018-2023 monitoring (Dashed line). Right: Graphs of variation between the depths of the average profiles and the PPEs. Positive (Negative) values in blue (Red) indicate that the average profile is at depths less (greater) than the PPE.

## 5. Discussion

For the interval after the dam failure, the results indicate the maintenance of the littoral drift and precipitation regimes in the drainage basin of the Doce River, but a reduction in the fluvial discharge. In response to this pattern, the coastline erodes near the mouth of the river. For the current period (2018-2023), the coastline continued to show erosion near the mouth, even with the increase in river discharge. The results of the morphodynamic monitoring of this region corroborate this erosion, since the measured profile is eroded in comparison to the PPE.

As in Sanchez *et al*. (2018) and Franco *et al*. (2024), the results presented provide an assessment of physical impacts on the beaches adjacent to the Doce River triggered by the arrival of mining tailings. These impacts have also been shown to be important in understanding the pattern of accumulation of chemical elements and the biological diversity of the coastal zone (Souza *et al*., 2022; Brahim *et al*., 2024).

The morphodynamics of the beaches along the deltaic plains of the Rio Doce are strongly controlled by exposure to waves and fluvial influence (Albino, Girardi and Do Nascimento, 2006; Albino and Suguio, 2010; Albino, Contti Neto and Oliveira, 2016; Albino; Girardi and Do Nascimento 2018). In this sense, the results point to the river discharge as the main causative agent of the changes observed after the dam failure, since this was the only one of the variables analyzed to demonstrate alteration. In addition, such a change shows no connection with the precipitation, since it also does not change over time. Thus, the reduction of river discharge after the dam

rupture was a result of the obstruction of the river flow, resulting from the deposition of mining tailings along the river channel (Vinzon *et al*., 2024).

The behavior of the coastline in the vicinity of the mouth is also strongly influenced by the patterns of river discharge found. In the period before the dam collapse, the river discharge levels promote sedimentary input. This sediment is reworked by littoral drift and the formation of sandy banks that migrate towards the continent, promoting progradation or stability of the coastline, in accordance with previous monitoring (Albino, Girardi and Do Nascimento, 2006; Albino, Contti Neto and Oliveira, 2016; Albino, Girardi and Do Nascimento, 2018; Rosa, 2023).

In addition to the reduction of discharge in the early stages of the arrival of the tailings at the coast, another important factor is the granulometry of this material. The iron ore tailings that reached the coastal region at later times represented a muddy sediment input (Do Carmo *et al*., 2017; Quaresma *et al*., 2020). The presence of mud in the foreshore region attenuates wave energy and is capable of generating a zone of deposition of sediments brought by the coastal drift, promoting progradation of the coastline (Wells and Roberts 1980; Roberts *et al*., 1989; Huh *et al*., 1991; Calliari *et al*., 2007). However, the results show that the preferential direction of the coastal drift does not favor the arrival of sediments in the vicinity of the mouth, on the contrary, it promotes the exit of sediments towards the north margin (Oliveira, Albino and Venancio, 2015) and restricts the arrival of sediments from the southern flank (Dominguez, 2006). Therefore, the attenuation of the competence of the waves by the presence of mud, reduces the formation and migration of the sandy banks towards the continent, thus triggering the retreat of the coastline. This process is more evident on the north bank of the mouth, due to the higher levels of mud transported by the coastal drift (Oliveira, Albino and Venancio, 2015; Vinzon *et al*., 2024). In addition, after the dam collapse, the reduction in river discharge reduces the depositional potential generated by the hydraulic jetty (Dominguez, Bittencourt and Martin, 1983), triggering the erosive process near the river mouth, also evidenced by Rosa (2023).

Wright and Short (1984) describe the morphological equilibrium of a sandy ocean beach as the balance between sediment and wave energy. During the 2020-2023 interval, river discharge returned to pre-dam failure levels, while wave-generated drift continued. However, the behavior of the coastline near the mouth follows an erosive pattern, as in the period after the breach. Our results suggest that the intensification of the retreat of the coastline near the mouth is a consequence of the granulometric and compositional alteration of the sediments, resulting from the current availability of mining tailings to the coastal zone (Vinzon *et al*., 2024.) The arrival of this material is evident from the increase in mud content and reduction in the average diameter of sediments on beaches between the years 2018 and 2023. The thinning of the sediment in the swash and surf zones reduces the slope of the emerged beach profile, intensifying the flooding process and favoring erosion. In contrast, the thinning of the sediment in the submerged region reduces the slope of the submerged profile, increasing the horizontal distance of sediment exchange and potentially reducing the height of the emerged beach (Hallermier, 1981; Bird, 2008; Short and Jackson, 2013; Davidson-Arnott, Bauer and Houser, 2019).

At the Mouth monitoring station, the accretion of the average profile in comparison with the PPE may be linked to filling of the submerged region by sedimentary input from the emerged beach, due to the thinning of the sediment from the swash and surf zones. The retreat of the coastline in this region corroborates this statement, illustrating the loss of sediment from the emerged beach to the submerged beach. On the north margin of the mouth, the erosive process of the coastline is in accordance with the flattening of the submerged region, following the behavior of the northern profile, which presents a reduction in the average diameter of the sediments and an increase in the mud content at 5 m depth.

The increase in river discharge between 2020 and 2023 also favors sedimentary deposition far from the coastline and greater depths, requiring greater wave energy for sediment reworking. The attenuation of the waves generated by the mud intensifies erosive processes along the coastline. The presence of mud also attenuates the littoral drift, reducing the action of the waves and trapping sandy sediments (Muehe *et al*., 2010), thus, cohesive muddy deposits tend to remain on the foreshore adjacent to the mouth of the Doce River, since they require high current velocities to be remobilized and transported (Hjulström, 1935; Van Rijn, 2007). This pattern is corroborated by the spatial limitation of the erosion of the coastline near the river mouth.

Located at the extremes of the study area, the North and South stations show stability and progradation of the coastline, emphasizing the reduction of fluvial influence with the distance from the mouth (Vespremeanu and Proeteasa, 2007; Hansen, Elias and Barnard, 2013; Anthony *et al*., 2017). At the North station, the stability of the

coastline is a function of the continuous sedimentary input transported by the littoral drift (Oliveira, Albino and Venancio, 2015). The accretion of the average profile compared to the PPE results from the arrival and deposition of fine sediments in the submerged region, marked by the inflection of the bathymetric profile beyond the depth of 9 m, probably delimiting the depth of closure (Hallermier, 1981). The erosive behavior of this profile up to 9 m depth may be linked to the presence of coarse sediment in the swash and surf zones (Albino and Suguio, 2010; Albino, Contti Neto and Oliveira, 2016), increasing the slope of the shallow foreshore and leaving this stretch of the middle profile deeper. Similarly, in the southern profile, the erosion in the average profile compared to the PPE can be attributed to the coarser grain size of the submerged region (Albino and Suguio, 2010; Albino, Contti Neto and Oliveira, 2016), conferring greater slopes and a deeper average profile. The stability of the coastline in this season is linked to the presence of sandy ridges and frontal dunes that represent a sedimentary source for the region (Albino, Girardi and Do Nascimento, 2006; Albino and Suguio, 2010). In addition, the results show inversions of the littoral drift near the mouth and a preferential drift to the south on the south bank of the Doce River, conferring the sedimentary contribution in this region. The reduction in the mud content of this station marks the strong transverse exchange of sediments, triggered by the high degree of exposure to waves (Albino and Suguio, 2010; Albino, Contti Neto and Oliveira, 2016).

## 6. Conclusions

The arrival of the mining tailings triggered erosive processes along the coastline adjacent to the mouth of the Doce River. The authors argue that the main mechanisms of this erosion are linked to: 1) Reduction of river discharge, caused by the retention of tailings along the river; 2) Attenuation of the migration of sandy banks towards the coastline, due to the contribution of muddy material and 3) Flattening of the beach profile, due to the reduction in grain size.

The effects of the contribution of muddy material on the mobility of the shoreline are inversely proportional to the distance from the mouth.

The erosion of the coastline adjacent to the mouth of the Doce River continues, even with the increase in river discharge. This dynamic, corroborated by the reduction in the average diameter of the sediments and by the PPE, demonstrates the current and continuous impact of the mud contribution on the beaches.

The mobility of the coastline corroborates the morphodynamic changes in the cross-sectional profiles, highlighting the multiscale characteristic of this study.

**Author Contributions:** Conception, B.E., M.N.Z. and J.A.; methodology, B.E. and P.J.; software, B.E. and P.J.; validation, J.A., P.J., G.M.V.M., L.B.C., L.H.S.O. and A.B.; data acquisition and preparation, B.E., M.N.Z., J.A., P.J., G.M.V.M., L.B.C., L.H.S.O. and A.B.; writing the article, B.E. and J.A.; review, J.A. and G.M.V.M.; supervision, J.A. All authors have read and agreed with the published version of the manuscript.

**Data availability:** We provide the dataset upon request to the corresponding author.

**Funding:** This research was funded by Aquatic Biodiversity Monitoring Program (PMBA), established by the Technical-Scientific Agreement (001/2018) between Federal University of Espirito Santo, Fundação Espirito-Santense de Tecnologia (FEST) and Renova Foundation.

**Acknowledgments:** The authors would like to thank the reviewers for their critical comments that improved the quality of this manuscript. Also, every student at the Laboratório de Geomorfologia Costeira e Sedimentologia da Universidade Federal do Espírito Santo (LAGES).

**Conflict of Interest:** The authors declare no conflict of interest. The funders had no interference in the development of the study; in the collection, analysis or interpretation of data; in the writing of the manuscript, or in the decision to publish the results.

**References**


1. ALBINO, J.; COELHO, A. L. N.; GIRARDI, G.; NASCIMENTO, K. A. D. In: MUEHE, D. C. E. H. Espírito Santo. Panorama da Erosão Costeira no Brasil. Brasília: Ministério do Meio Ambiente. 433-478. 2018.
2. ALBINO, J.; GIRARDI, G.; NASCIMENTO, K. A. D. Espírito Santo. *Erosão e progradação do litoral brasileiro. Brasília: MMA*, 227-264. 2006.
3. ALBINO, J.; NETO, N. C.; OLIVEIRA, T. C. A. The Beaches of Espírito Santo. *In:* SHORT, A. D.; KLEIN, A. H. D. F. (Ed.). *Brazilian beach systems*. Springer, p. 333-361. 2016.
4. ALBINO, J.; SUGUIO, K. Sedimentation processes and beach morphodynamics active at the Doce River mouth, Espírito Santo State, Brazil. *Anais da Academia Brasileira de Ciências*, *82*, 1031-1044. 2010.
5. ANTHONY, E. J.; DUSSOUILLEZ, P.; DOLIQUE, F.; BESSET, M.; BRUNIER, G.; NGUYEN, V. L.; GOICHOT, M. Morphodynamics of an eroding beach and foredune in the Mekong River delta: Implications for deltaic shoreline change. Continental Shelf Research 147, p 155-164. 2017.
6. BAIG, M. R. I.; AHMAD, I. A.; SHAHFAHAD, TAYYAB, M.; RAHMAN, A. Analysis of shoreline changes in Vishakhapatnam coastal tract of Andhra Pradesh, India: an application of digital shoreline analysis system (DSAS). *Annals of GIS*, *26*(4), 361-376. 2020.
7. BASCOM, W. N. The relationship between sand size and beach-face slope. *Eos, Transactions American Geophysical Union*, *32*(6), 866-874. 1951.
8. BIRD, E. C. *Coastal geomorphology: an introduction*. John Wiley & Sons. 2008.
9. BITTENCOURT, A. C.; DOMINGUEZ, J. M.; MARTIN, L.; SILVA, I. R.; DE-MEDEIROS, K. O. Past and current sediment dispersion pattern estimates through numerical modeling of wave climate: an example of the Holocene delta of the Doce River, Espírito Santo, Brazil. *Anais da Academia Brasileira de Ciências*, *79*, 333-341. 2007.
10. BOAK, E. H.; TURNER, I. L. Shoreline definition and detection: a review. *Journal of coastal research*, *21*(4), 688-703. 2005.
11. BRAHIM, S.; SOBRINHO, T. G.; ALBINO, J.; ZANETTI, G.; DO AMARAL, V. S.; CARNEIRO, M. T. W.; DA COSTA, K. G. Benthic fauna along sandy beaches enriched by metals after mining disaster. *Marine Ecology Progress Series*, *726*, 181-196. 2024.
12. CALLIARI, L. J.; HOLLAND, K. T.; PEREIRA, P. S.; GUEDES, R. M.; SANTO, R. E. The influence of mud on the inner shelf, shoreface, beach, and surf zone morphodynamics—Cassino, Southern Brazil. In *Coastal Sediments' 07* (pp. 1455-1465). 2007.
13. COSTA, E. S.; CAGNIN, R. C.; DA SILVA, C. A.; LONGHINI, C. M.; SÁ, F.; LIMA, A. T.; NETO, R. R. Iron ore tailings as a source of nutrients to the coastal zone. *Marine Pollution Bulletin*, *171*, 112725. 2021.
14. COSTA, P. G.; MARUBE, L. C.; ARTIFON, V.; ESCARRONE, A. L.; HERNANDES, J. C.; ZEBRAL, Y. D.; BIANCHINI, A. Temporal and spatial variations in metals and arsenic contamination in water, sediment and biota of freshwater, marine and coastal environments after the Fundão dam failure. *Science of The Total Environment*, *806*, 151340. 2022.
15. CUPOLILLO, F.; DE ABREU, M. L.; VIANELLO, R. L. Climatologia da bacia do rio Doce e sua relação com a topografia local. *Revista Geografias*, *4*(2), 45-60. 2008.
16. DAVIDSON-ARNOTT, R.; BAUER, B.; HOUSER, C. *Introduction to coastal processes and geomorphology*. Cambridge university press. 2019.
17. DEAN, R. G. Equilibrium beach profiles: characteristics and applications. *Journal of coastal research*, 53-84. 1991.
18. DIRETORIA DE HIDROGRAFIA E NAVEGAÇÃO (DHN). Centro de hidrografia da marinha. Banco nacional de dados oceanográficos. Previsões de maré. Disponível em: http://www.mar.mil.br. Acesso em: 20 mar. 2025.
19. DO CARMO, F. F.; KAMINO, L. H. Y.; JUNIOR, R. T.; DE CAMPOS, I. C.; DO CARMO, F. F.; SILVINO, G.; PINTO, C. E. F. Fundão tailings dam failures: the environment tragedy of the largest technological disaster of Brazilian mining in global context. *Perspectives in ecology and conservation*, *15*(3), 145-151. 2017.
20. DOMINGUEZ, J. M. L. The coastal zone of Brazil: an overview. Journal of Coastal Research, 16-20. 2006.
21. DOMINGUEZ, J. M. L.; BITTENCOURT, A. C. S. P.; MARTIN, L. O papel da deriva litorânea de sedimentos arenosos na construção das planícies costeiras associadas às desembocaduras dos rios São Francisco (SE/AL), Jequitinhonha (BA), Doce (ES) e Paraíba do Sul (RJ). *Revista Brasileira de Geociências*, *13*(2), 98-105. 1983.

22. EGUCHI, B. M. M.; KLUMB-OLIVEIRA, L. Clima de ondas de tempestades na costa brasileira utilizando 41 anos de dados da reanálise ECMWF ERA5. *Revista Brasileira de Climatologia*, *32*, 544-565. 2023.
23. FRANCO, T.; ZORZAL-ALMEIDA, S.; SÁ, F.; BIANCHINI, A.; DERGAM, J. A.; ESKINAZI-SANT'ANNA, E. M.; BASTOS, A. C. Ex-post impact assessment on a large environmental disaster. *Environmental challenges*, *15*, 100889. 2024.
24. GHARNATE, A.; TAOUALI, O.; MHAMMDI, N. Shoreline Change Assessment of the Moroccan Atlantic Coastline Using DSAS Techniques. *Journal of Coastal Research*, *40*(2), 418-435. 2024.
25. GILBERT, R. O. *Statistical methods for environmental pollution monitoring*. John Wiley & Sons. 1987.
26. HALLERMEIER, R. J. A profile zonation for seasonal sand beaches from wave climate. *Coastal engineering*, *4*, 253-277. 1981.
27. HANSEN, J. E.; ELIAS, E.; BARNARD, P. L. Changes in surfzone morphodynamics driven by multi-decadal contraction of a large ebb-tidal delta. Marine Geology 345, p. 221-234, 2013.
28. HERSBACH, H.; BELL, B.; BERRISFORD, P.; HIRAHARA, S.; HORÁNYI, A.; MUÑOZ-SABATER, J.; THÉPAUT, J. N. The ERA5 global reanalysis. *Quarterly journal of the royal meteorological society*, *146*(730), 1999-2049. 2020.
29. HJULSTRÖM, F. *Studies of the morphological activity of rivers as illustrated by the River Fyris* (Doctoral dissertation, The Geological institution of the University of Upsala). 1935.
30. HUH, O. K.; ROBERTS, H. H.; ROUSE, L. J.; RICKMAN, D. A. Fine grain sediment transport and deposition in the Atchafalaya and Chenier Plain sedimentary system. 1991.
31. KAMPHUIS, J.W. Alongshore transport of sand. Proceedings of the 28th International Conference on Coastal Engineering, American Society of Civil Engineers, Cardiff, Wales, 2478-2490. 2002.
32. KARUNARATHNA, H.; HORRILLO-CARABALLO, J.; KURIYAMA, Y.; MASE, H.; RANASINGHE, R.; REEVE, D. E. Linkages between sediment composition, wave climate and beach profile variability at multiple timescales. *Marine Geology*, *381*, 194-208. 2016.
33. LE MÉHAUTÉ, B.; KOH, R. C. Y. On the breaking of waves arriving at an angle to the shore. *Journal of Hydraulic Research*, *5*(1), 67-88. 1967.
34. LOPES, J. R. F.; SILVA, D. D. Aplicação do teste de Mann-Kendall para análise de tendência pluviométrica no estado do Ceará. *Revista de Geografia (Recife)*, *30*(3), 192-208. 2013.
35. MARQUES, J. A.; COSTA, S. R.; MARASCHI, A. C.; VIEIRA, C. E.; COSTA, P. G.; MARTINS, C. D. M. G.; BIANCHINI, A. Biochemical response and metals bioaccumulation in planktonic communities from marine areas impacted by the Fundão mine dam rupture (southeast Brazil). *Science of the Total Environment*, *806*, 150727. 2022.
36. MUEHE, D., SPERLE, M., TESSLER, M. G., & SOUZA, S. R. Can the trapping of shoreface sand by mud layers induce coastal erosion? The example of the Paraiba do Sul river outlet, Northern Rio de Janeiro state. *Brazilian Journal of Oceanography*, *58*, 65-68. 2010.
37. OLIVEIRA, K. S. S.; DA SILVA QUARESMA, V. Temporal variability in the suspended sediment load and streamflow of the Doce River. *Journal of South American Earth Sciences*, *78*, 101-115. 2017.
38. OLIVEIRA, T. C. A.; ALBINO, J.; VENANCIO, I. Transporte longitudinal de sedimentos no litoral da planície deltaica do Rio Doce. *Quaternary and Environmental Geosciences*, *6*(1), 20-25. 2015.
39. PIANCA, C.; MAZZINI, P. L. F.; SIEGLE, E. Brazilian offshore wave climate based on NWW3 reanalysis. *Brazilian Journal of Oceanography*, *58*, 53-70. 2010.
40. QUARESMA, V. S.; BASTOS, A. C.; LEITE, M. D.; COSTA JR, A.; CAGNIN, R. C.; GRILO, C. F.; OLIVEIRA, K. S. S. The effects of a tailing dam failure on the sedimentation of the eastern Brazilian inner shelf. *Continental Shelf Research*, *205*, 104172. 2020.
41. RICHARD, E. D. C.; ESTRADA, G. C. D.; BECHTOLD, J. P.; DE AGUIAR DUARTE JR, H.; MAIOLI, B. G.; DE FREITAS, A. H. A.; FIGUEIREDO, L. H. M. Water and sediment quality in the coastal zone around the mouth of Doce River after the Fundão tailings dam failure. *Integrated Environmental Assessment and Management*, *16*(5), 643-654. 2020.
42. ROBERTS, H. H.; HUH, O. K.; HSU, S. A.; ROUSE JR, L. J.; RICKMAN, D. A. Winter storm impacts on the chenier plain coast of southwestern Louisiana. 1989.
43. ROSA, M.F. Mapeamento da mobilidade da linha de costa adjacente à desembocadura do rio Doce-ES, entre 2007-2021. Monografia – Universidade Federal do Espírito Santo, Vitória, 2023.

44. SÁNCHEZ, L.E.; ALGER, K.; ALONSO, L.; BARBOSA, F.A.R.; BRITO, M.C.W.; LAUREANO, F.V.; MAY, P.; ROESER, H.; KAKABADSE, Y. Impacts of the Fundão Dam failure. A pathway to sustainable and resilient mitigation. Rio Doce Panel Thematic Report No. 1. Gland, Switzerland: IUCN. 2018.
45. SANTOS, D. N. D.; DA SILVA, V. D. P.; SOUSA, F. D. A.; SILVA, R. A. Estudo de alguns cenários climáticos para o Nordeste do Brasil. *Revista Brasileira de Engenharia Agrícola e Ambiental*, *14*, 492-500. 2010.
46. SCHETTINI, C. A.; HATJE, V. The suspended sediment and metals load from the Mariana's tailing dam failure to the Coastal Sea. *Integrated Environmental Assessment and Management*, *16*(5), 661-668. 2020.
47. SHORT, A. D.; JACKSON, D. W. T. Beach morphodynamics. *Treatise on geomorphology*, 106-129. 2013.
48. SILVA, C. V. V.; ALMEIDA, J. R.; SILVA, C. E.; CARVALHO, L. O.; SILVA, C. D. Physical-chemical monitoring of the linhares (es) and são mateus (es) aquatic ecosystem after the breaking of the fundão dam, mariana, minas gerais. In *OPEN SCIENCE RESEARCH I* (Vol. 1, pp. 273-286). Editora Científica Digital. 2022.
49. SILVESTER, R.; HSU, J. R. *Coastal stabilization* (Vol. 14). Singapore: World Scientific. 1997.
50. SOUZA, J. R.; SIELSKI, L. H.; KRAUSE, M.; SOUZA, B. S.; BRANDÃO, G. P.; ALBINO, J.; CARNEIRO, M. T. W. D. The influence of beach geology and morphodynamics on chemical pollution assessments following a mining accident. *Marine Pollution Bulletin*, *174*, 113230. 2022.
51. THIELER, E. R.; DANFORTH, W. W. Historical shoreline mapping (I): improving techniques and reducing positioning errors. *Journal of Coastal Research*, 549-563. 1994.
52. VAN RIJN, L. C. Unified view of sediment transport by currents and waves. I: Initiation of motion, bed roughness, and bed-load transport. *Journal of Hydraulic engineering*, *133*(6), 649-667. 2007.
53. VESPREMEANU-STROE, A.; PREOTEASA, L. Beach–dune interactions on the dry–temperate Danube delta coast. *Geomorphology*, *86*(3-4), 267-282. 2007.
54. VIEIRA, F. V.; BASTOS, A. C.; QUARESMA, V. S.; LEITE, M. D.; COSTA JR, A.; OLIVEIRA, K. S.; AMADO FILHO, G. M. Along-shelf changes in mixed carbonate-siliciclastic sedimentation patterns. *Continental Shelf Research*, *187*, 103964. 2019.
55. VINZON, S. B.; GALLO, M. N.; GABIOUX, M.; FONSECA, D. L.; ACHETE, F. M.; GHISOLFI, R. D.; MACHADO, L. G. The role of waves in the resuspension and transport of fine sediment and mine tailings from the Fundão Dam failure, Doce River, Brazil. *International Journal of Sediment Research*, *39*(1), 44-60. 2024.
56. WELLS, J. T.; ROBERTS, H. H. Fluid mud dynamics and shoreline stabilization: Louisiana chenier plain. In *Coastal Engineering* (pp. 1382-1401). 1980.
57. WRIGHT, L. D.; SHORT, A. D. Morphodynamic variability of surf zones and beaches: a synthesis. *Marine geology*, *56*(1-4), 93-118. 1984.